Energy & Environmental Science

ROYAL SOCIETY OF CHEMISTRY

PAPER

View Article Online
View Journal | View Issue

Cite this: *Energy Environ. Sci.*, 2024, **17**, 5639

Designed-by-purpose power sources: a cardboard primary battery for smart packaging†

Marina Navarro-Segarra, *[ab] Omar A. Ibrahim,[c] Iñigo Martin-Fernandez,[b] Carles Tortosa,[bc] Joseba M. Ormaetxea,[b] Manuel Baumann,[d] Marcel Weil[de] and Juan Pablo Esquivel *[abf]

Internet-of-Things (IoT) is considered one of the primary enablers of the next digital transformation wave. Generating and exchanging data between the increasing number of delocalized sensors comes with the need for high-performance portable power sources that also meet environmental and social responsibility standards. This article presents a portable power source to meet the energy requirements of IoT devices in the smart packaging sector that has been designed-by-purpose in an ecologically benign way since the early development stage. To minimize the environmental impact throughout its life cycle, the battery follows the value chain of paper and cardboard, from material sourcing to disposability. Naturally abundant materials, such as cellulose derivates and alginate biopolymers, are prioritized to create the separator and contain the redox species. Manufacturing techniques, easily implementable in the packaging industry, are used to fabricate an adhesive label-like battery (based on layered components) and engrave the current collectors, *via* laser-induced graphene. The prototype's energy adaptation capability is demonstrated by directly powering two applications particularly appealing for smart packaging, *i.e.*, a printed electrochromic display and a wireless tracker device. Once depleted, the battery is compatible with paper and cardboard recycling standardized processes. The reconceptualization of the whole battery life cycle leads to the generation of a disruptive power source concept that aims to be an enabler of a sustainable digitalization of society.

Received 19th January 2024,
Accepted 11th June 2024

DOI: 10.1039/d4ee00306c

rsc.li/ees

Broader context

Digital technologies have gained an essential role in societies' development, by generating global changes in economic, social, and environmental dimensions. Instant access to information and education has contributed to the transformation of lifestyles and business models. In this evolving scenario, the so-called Internet-of-Things (IoT) is considered one of the primary enablers of the next digital transformation wave; together with big data analytics and artificial intelligence. However, boosting the interconnectivity and generating and sending sensor data requires a significant sum of electrical and electronic devices and their associated power sources. This demand for portable energy must be fulfilled by power sources with high performance, but they should also possess environmental sustainability and social responsibility. In this work, smart packaging is selected as a blooming sector to present a designed-by-purpose battery to power IoT devices. The article provides a concise view of the energy needs of increasingly digitalized products and services, the environmental concerns of current portable power sources and how the proposed technology broadens the edges of portable power solutions in terms of sustainability combined with useful performance metrics, offering a profitable design approach to address future society's technological needs from a just and safe space.

[a] *BCMaterials, Basque Centre for Materials, Applications and Nanostructures, UPV/EHU Science Park, 48940 Leioa, Spain. E-mail: marina.navarro@bcmaterials.net, juanpablo.esquivel@bcmaterials.net*
[b] *Instituto de Microelectrónica de Barcelona, IMB-CNM (CSIC), C/dels Til·lers sn, Campus UAB, 08193 Bellaterra Barcelona, Spain*
[c] *Fuelium S.L., Edifici Eureka, Av. Can Domènech S/N, 08193 Bellaterra, Barcelona, Spain*
[d] *ITAS, Institute of Technology Assessment and Systems Analysis, KIT – Karlsruhe Institute for Technology, Karlsruhe, Germany*
[e] *HIU, Helmholtz Institute Ulm for Electrochemical Energy Storage, Ulm, Germany*
[f] *IKERBASQUE, Basque Foundation for Science, 48009 Bilbao, Spain*

† Electronic supplementary information (ESI) available: Scenarios for battery-powered IoT devices in smart packaging, associated materials and energy consumptions, packaging industry and label fabrication methods, figures on LIG patterning, additional figures on LIG electrical and morphological studies, prototype components exploded view. See DOI: https://doi.org/10.1039/d4ee00306c

1. Introduction

As the dependence of societies on digital technologies speeds up, most products' life cycles become shorter; consequently, technological innovations are accompanied by an ever-increasing amount of waste.[1–3] The discarded electrical and electronic equipment (namely, e-waste or WEEE) is the world's fastest-growing solid-waste stream, with 53.6 Mt generated in 2019 according to the Global E-waste Monitor 2020.‡ Furthermore, electronics is one of the major world consumers of metals, such as gold, silver, lead, cobalt, nickel, cadmium or copper; thus, e-waste contains equally hazardous and valuable materials.[4,5] Countries and organizations are endeavouring towards e-waste management. However, the documented global percentage of collected and properly recycled WEEE in 2019 was only 17.4%, meaning that the large majority of e-waste generated was not formally collected nor systematically managed. When properly collected, only the high-value components are recovered (whereas the low-value materials are simply disposed of in landfills or incinerated). Still, their complex design and material heterogeneity make this process very time-consuming and energy-intensive.[6–8] Consequently, from an economic and environmental perspective, the noteworthy efforts associated with collection and recycling are only weighted in a few specific recovered product cases, as demonstrated by Peters *et al.*[9] This casts doubts on whether the reward associated with the collection and recycling of all WEEE materials is justified when efforts are excessively high and not justified by the environmental impacts mitigation.

On top of that, the societal dependence on electronics is expected to worsen with the rise of Internet of Things (IoT) solutions. IoT is considered one of the primary enablers of the next digital transformation. It has already penetrated various markets such as agriculture, transport, smart city or healthcare.[10,11]

In this scenario, portable batteries play an essential role due to their capability to deliver high energy densities in a lightweight and compact format. However, their value chain presents analogous environmental and ethical drawbacks to WEEE's. Energy storage technologies still rely on hazardous and non-sustainable compounds as defined in JRC Technical Report 'Safe and Sustainable by Design chemicals and materials', sometimes even obtained from unethical supply chains (*e.g.* through artisanal mining and child labour).[12–14] These materials include heavy metals and/or toxic chemicals (*e.g.*, lithium, cadmium, manganese, copper, zinc, cobalt, *etc.*) that are highly detrimental to the ecosystems in case of leakage during their operational lifespan or improper management at their End of Life (EoL).[15,16] Numerous studies exist on the environmental performance and management strategies of spent battery flows.[16–21] However, despite the considerable efforts performed through environmental policies, recycling rates are hardly met. The ongoing policies planned for repurposing and recycling of large-scale batteries are not directly applicable to portable power sources, because of the strong dependence on the diverse variety of use case scenarios, the user self-responsibility and the availability of collection infrastructures. In the EU, statistics show that from the 229 kilotons of portable batteries sold in 2020, the collection rate was only 47%, a 4.4% decrease compared to 2019. The current EU Batteries Regulation (2023/1542) sets ambitious collection targets for portable batteries (45% for 2023, 63% for 2027, and 73% for 2031), posing a significant challenge for most EU countries; and deemed a hardly reachable attainment at a global level.[22,23] In addition, the regulation also aims reducing the carbon footprint of battery manufacturing, improve the ethical sourcing of raw materials and to enhance the security of supply.

Further digitalization of products and services should not come at the cost of an additional uncontrollable electronic waste burden (including batteries). Such concern becomes especially alarming in sectors such as packaging, that are undergoing deep transformations driven by the change in consumer trends and the blooming of e-commerce.[24,25] For example, different electronic systems such as trackers, sensors, displays, or communication modules are progressively being incorporated into the packaging supply chain to ensure efficient logistics and an improved customer experience. These IoT systems are known as smart packaging solutions and are intended to add many advantages to the packaging industry at economic and sustainable levels.[26,27]

Powering smart packaging solutions – and IoT systems in general – demands advanced integrated single-use batteries. Conversely, primary battery technology has not experienced significant innovations in the last decades. Given their exceptional performance, compactness and significant operational time, systems such as Zn or Li coin cells or alkaline cells have dominated the market over the years.[28] These cells, however, suffer from a lack of format-adaptability resulting in a concerning dissociation between the application's energy requirements and the energy stored in the battery, which leads to an inefficient use of resources. In this context, printed batteries have emerged as an alternative technology for the fabrication of batteries on a wide variety of substrates, from plastic films to paper or metals. Printed batteries have successfully bypassed conventional technology format constraints, providing new functionalities such as flexibility, form versatility and lightweight; in a simple and low-cost manner.[29,30] Nevertheless, these cells do not offer an overall sustainable solution, because the technology still relies upon conventional materials, such as currently controversial petroleum-based substances known as per- and poly-fluoroalkyl (PFAS). Metals for the cathode (Mo, Au, Pd, MnO_2), anode (Zn, Li, Mn), and current collectors (Al, Cu) are the most common materials, together with petroleum-based polymers for the separator or the casing.[29] The use of critical raw materials, *e.g.* Li, Au, represent a challenge for safe supply chains for battery technologies in Europe.[31] Beyond that, the use of hazardous materials is also being addressed

‡ For the reader to be aware of the magnitude of the issue, the authors highly recommend the work 'CTRL-X' from the photographer Kai Löffelbwin 'A topography of e-waste' together with 'The e-waste mountains – in pictures' article from The Guardian.

in the new Batteries Regulation (2023/1542) and has led to the development of corresponding assessments.[32,33] These aspects have led to a set of policy measures and a wider public debate.[22,34] Consequently, named drawbacks hamper the spread of more efficient and environmentally sustainable IoT solutions.

This work presents a 'fit-for-purpose' battery approach designed for smart packaging applications. This primary battery concept turns around the typical battery life cycle, covering the industry's prospective needs with an environmentally conscious solution: the employed fabrication methods could be seamlessly integrated into standard packaging protocols and its sticker-like design allows to practically attach it to a generic cardboard box (or envelope) surface. The new battery concept is based on abundant renewable biopolymers with a water-based chemistry, thus hazardous or toxic materials have been deliberately avoided. Despite being at a low technology readiness level, the battery prototype has demonstrated its applicability by powering two practical, real-world applications, that are exemplary within the packaging sector, an E-paper display and a tracker device. Finally, the power source has been proven to be compatible with paper and cardboard recycling processes under the standardized protocols used in the industry.

2. Results and discussion

2.1 Battery design under a life cycle thinking approach

In some application niches, IoT solutions might intrinsically generate higher environmental impacts. For instance, those in which due to the sector logistics the IoT system ends up distributed widespread, resulting in an increase in the responsibility level for the end user to properly discard/re-use the system. For this reason, the packaging sector was selected in this work to evidence the importance of analyzing the specific niche of application when developing a portable power source. Different scenarios for conventional battery-powered IoT devices in smart packaging were drafted to identify possible outcomes of the batteries after their operational lifetime (see ESI†). These scenarios include a range in the implementation level of good practices, user responsibility and proper waste management. A 'worst-case' scenario (named as C) describes a case in which the proliferation of IoT devices in packages could lead to a significant disturbance in the paper recycling system (due to the compelled rejection of cardboard boxes including conventional batteries), causing an unwanted reduction of cardboard circularity and recycling rates. This scenario is the one selected as framework for the present approach, in which the power source is designed-by-purpose for IoT devices in the smart-packaging sector. Accordingly, during the power source conceptualization, the application is used as the linchpin to guide the life cycle thinking process by which the entire battery value chain is reformulated – from the raw materials selection and the necessary energy for the battery fabrication, through its distribution, use and final disposal.[24,35,36] In Fig. 1 a holistic representation is shown of the envisioned prototype together with its geometry, parts, life cycle thinking methodology and operation principle. Ideally, a prospective life cycle assessment approach is required to validate the benefits of the prototype. However, providing robust assessments requires a thoroughly consideration of various impact categories and consideration of all life cycle phases entailing resource extraction, processing, manufacturing, use and end-of-life aspects.[37] This comes, in particular, true for the targeted application in the packaging industry where high waste streams exist. In addition, our prototype is based on a laboratory scale requiring a theoretical upscaling,[38] of our processes, to assure comparability and robustness of potential environmental benefits, which is beyond the scope of this work. However, as the first step all relevant material and energy flows are provided in the Fig. S1 (ESI†), serving as a starting point for corresponding assessments. In order to minimize the overall battery impacts, its life cycle is planned in consonance with that of the host product, *i.e.*, a cardboard package. The recent European Batteries Regulation already adopts a holistic approach to establish requirements for sustainable battery development throughout their complete life cycle.[22] This regulation covers power sources in superior TRL stages and made from conventional materials advocating for dedicated EoL management. The prototype presented herein is believed to potentially fit in the key points established by the regulation, such as ''production with the lowest possible environmental impact, using materials that have been obtained in full respect of social and ecological standards''. Doing so, allows to tackle the most recent regulations towards mandatory battery labelling from very early cell development. However, it is worth mentioning that coupling battery repurposing with its host product', is not yet considered by this battery norm.

Following a life-cycle planning process, the potential creation of environmental stress at each stage is taken as a decisive driver to guide the battery design.[39,40] Naturally abundant and non-toxic materials have been consciously selected for all battery parts, from the substrate to the active redox species, actively prioritizing material compatibility with the packaging sector. Hence, materials selection has been carried out considering the EN643:2001 Paper and cardboard-European list of standard grades of paper and cardboard standard specifications, which clearly defines the tolerances for unwanted, and prohibited, materials during paper recycling. Conventional metal-based energy storage materials have been deliberately avoided. Low-impact fabrication techniques that could be coupled with the fabrication methods in the packaging industry are proposed as key feature to minimize the overall ecological footprint and to directly avoid the distribution stage. For the use stage, the prototype was conceived as a power source with energy-adaptable capabilities. Finally, it could be directly repurposed with paper and cardboard without disturbing this waste stream. The end-of-life proposed is a disruptive strategy to mitigate the environmental costs of digitalization in the EoL stage hot spot. This approach seeks the creation of a close loop, in which the low-value materials are directly repurposed by taking advantage of the host product's well-established waste

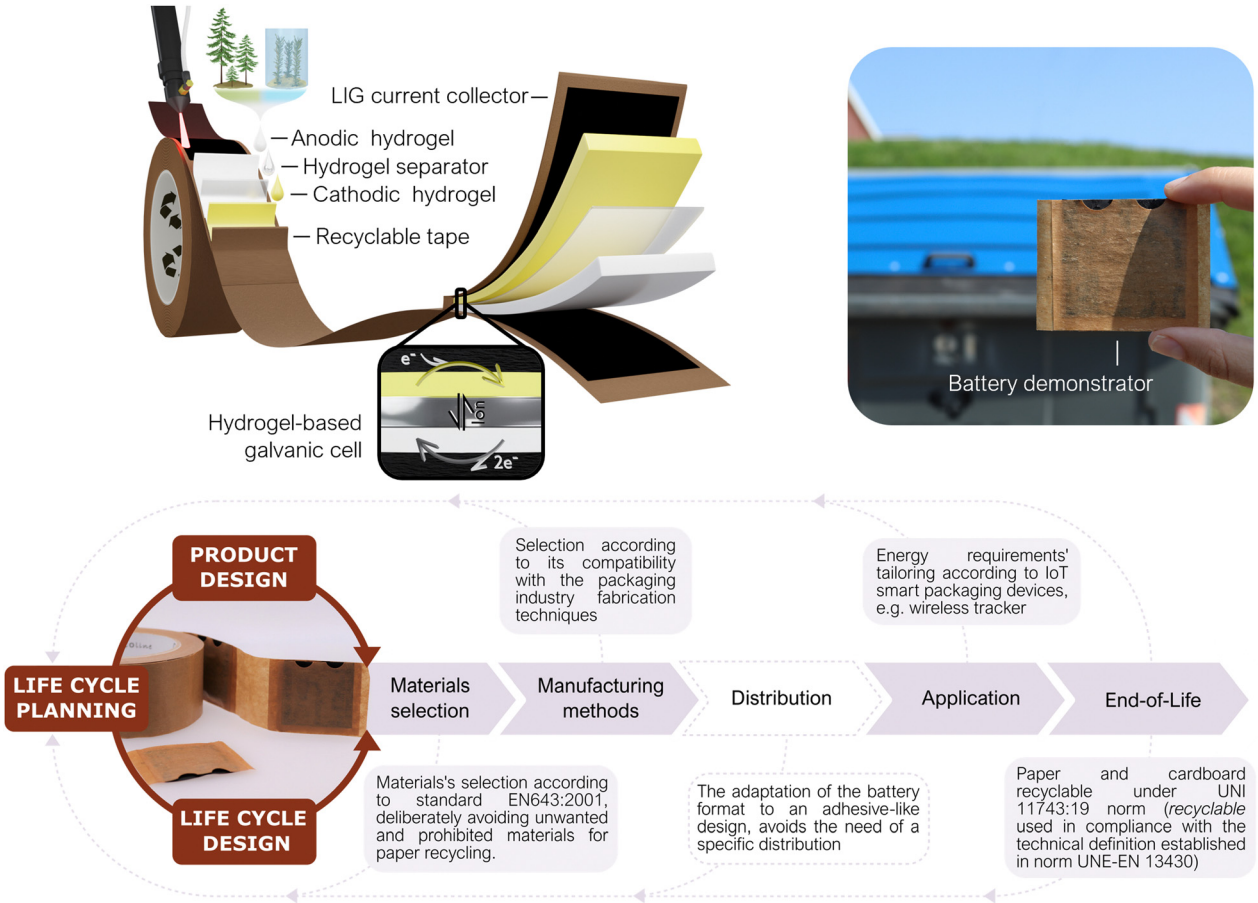

Fig. 1 Prototype evolution from holistic envisioning to the functional battery in an adhesive label format. Tailored for smart packaging applications, battery fabrication is based on low-impact techniques: laser-induced graphene technique is used to engrave the current collectors on top of a precursor and bio-based abundant materials derived from wood and algae, are used to create the gelified battery layers. The battery design, based on self-standing layered hydrogels enhances the demonstrator compatibility with smart packaging industry and allows a fit-for-purpose energy format. Finally, due to its unique material composition, the demonstrator can be recycled along with cardboard boxes at its end-of-life. The representation of the systematic methodology followed for the life cycle planning has been adapted from Umeda *et al.* 2012.

streams. Therefore, the need for separate collection and treatment routes is overcome; which in the case of portable batteries, highly rely on end-consumer responsibility (see in ESI†). The main disadvantage of this EoL scenario is that, although the recycled battery might become paper/cardboard pulp to be repurposed into another box or package, the electroactive materials are not easily recoverable to produce another battery. But on the other side, as already mentioned, no efforts for collection, separate transport and recycling are necessary, thus directly avoiding the associated harmful impacts to the environment.

Geometrically, the battery has a label-like rectangular structure, meaning it is a planar prototype composed of a set of layers with different purposes. Two layers of pretreated cardboard tape act as both structural material and substrate over which carbon-based current collectors are generated *via* the laser-induced graphene (LIG) technique. According to EU Chemicals Strategy for Sustainability (2020), the use of safe and non-toxic bio-based materials as the battery matrix and a water-based chemistry has been prioritized to ensure the harmfulness of the power source in case of any damage or leakage.[41] The electroactive compounds are contained in an ionically conductive hydrogel matrix that acts as an electrolyte backbone. The hydrogel, composed of naturally occurring polymers (cellulose and alginate), is used to create gelified self-standing anodic and cathodic reservoirs. Finally, the biopolymeric membrane is also used as the separator, and sandwiched between the anode and cathode, to avoid short circuits and allow the ionic exchange (see Fig. 1). The preparation of each layer is done separately and the battery is assembled through a sheet lamination process. This approach facilitates the battery manufacturing implementation into a cardboard box production line as explained in Fig. S2 (ESI†).

2.2. Battery materials

2.2.1. Laser-induced graphene as battery current collector. Current collectors have a crucial influence on the performance of batteries. Characteristics such as electrical conductivity, contact resistance, density or corrosion resistance, directly affect the capacity and efficiency of the battery. The most

commonly used current collectors in batteries are metals (Al, Cu, Ni, Ti, or stainless steel) due to their high electrical conductivity, electrochemical stability, and mechanical strength. However, metallic current collectors' suitability raises concerns due to their non-renewable nature, increasing economic (and environmental) costs and sustainability implications.[42] In this sense, carbon-based current collectors (*e.g.* carbon papers, carbon felts, or nanocarbons) could overcome metal-based drawbacks while meeting essential requirements.[43–45] Nanocarbon materials, *i.e.* carbon nanotubes and graphene, have attracted intense research interest because of their outstanding characteristics as electrical conductors.[46] However, despite its extraordinary properties, graphene-wide application in commercial devices has been sluggish, mainly because high-end applications demand a single or few graphene layers, and this still requires breakthroughs to overcome the economic and environmental costs of their solution-based processing.[47,48]

In 2014, J. Lin *et al.* discovered that direct lasing with a CO_2 infrared laser on a commercial polyimide generated 3D porous and conductive graphene on the film (see Fig. S3, ESI†).[49] The so-called laser-induced graphene (LIG) technique is striking because it combines 3D graphene preparation and patterning into a single step. This approach widens graphene application niches (*i.e.* sensing and energy storage fields). Since, it enables graphene creation under a selective patterned area by direct laser scribing on a precursor material; avoiding the need for intermediate chemicals with only a commercial CO_2 laser system and minimal residue generation.[50–54]

LIG formation on cardboard has already been successfully reported by using a flame-retardant surface treatment before the definition of LIG structures.[53] Within this work two of these commercial pretreatments (Phosphate ammonium-based Force-Field® FireGuard (FG) and boric acid-based FireChief® Flame Retardant Spray (FRS)) were evaluated against a newly developed bio-inspired pretreatment. The bio-based approach was developed with two purposes. First, to act as a flame retardant with an environmentally safer chemical composition; since it is composed of cellulose and lignin using water as a solvent. Second, to increase the lignin content on the substrate surface which, according to the literature, improves LIG quality (see ESI,† Fig. S3).[55–58] This lignin-based precursor material can be used as a bio-based coating if poured on top of a cardboard substrate or as a self-standing membrane. As explained below, in this work the bio-based precursor has been used as coating for cardboard during LIG optimization and concept validation. Then it is used as self-standing membrane for the final battery prototype. Finally, Kapton® polyimide (PI) was chosen as benchmark to produce LIG and compare performance, as its use as precursor has been widely reported.

Once the precursors were defined, the specific laser conditions for each substrate were optimized. Fig. S3 (ESI†) illustrate a summary of the engraving parameters specifically assessed within this study together with an example of the matrix condition method used as a tool for lasing conditions screening. Speed of the laser (*S*), its power (*P*) and defocus were the variable parameters screened in this study. Regarding the working atmosphere, ambient conditions were used. Furthermore, in this work, defocus was prioritized above consecutive lasing, as an energy-saving strategy especially relevant for process scale-up. It is important to emphasize that small percentile units of laser speed and power make a crucial difference between obtaining LIG and perforating the substrate or not modifying it at all. Thus, to export the technique onto the precursors of interest a matrix-based procedure was used (see Fig. S3, ESI†).

S–P working range was iteratively adapted and narrowed until the LIG-yielding conditions were found for each precursor. To summarize, PI and LIGNIN precursors are converted into LIG in a single lasing step without the need for defocusing. While, regarding the cardboard pretreated with FS and FRS, 3 mm of defocusing distance was required to produce the LIG in a single lasing step. The *S–P* conditions producing homogenous LIG were then used to evaluate their electrical suitability. The conditions generating the most electrically conductive LIG were then characterized electrochemically and morphologically.

2.2.2. Engraving conditions screening *via* electrical characterization. The Van der Pauw method was used to determine sheet resistance (R_s), see eqn (S1) (ESI†). Notice that LIG materials have intrinsic anisotropy due to the direction of the laser rastering. To assess the relevance of this property, sheet resistance was evaluated parallel to the raster direction and perpendicular to it, thus obtaining two R_s values, $R_{s,\parallel}$ and $R_{s,\perp}$ (see Fig. S3f, ESI†). Fig. S4 (ESI†) presents the $R_{s,\parallel}$ and $R_{s,\perp}$ of FRS, FG and LIGNIN precursors converted into LIG at the corresponding combination of *S–P* conditions.

The best-performing lasing conditions in terms of electrical conductivity, *i.e.* lowest sheet resistance values, were further studied. Depicted in Fig. 2a and b can be found the LIG-generating conditions found for each studied precursor material and their respective R_s values. Fig. 2c contains optical images of the precursor materials before and after lasing with different *S–P* combinations, including the successful generation of LIG, *i.e.* $R_{s,\parallel} < 50\ \Omega\ sq^{-1}$.

As it can be observed, LIG shows strong conductivity anisotropy, meaning that for the same lasing conditions $R_{s,\perp}$ is at least one order of magnitude higher than $R_{s,\parallel}$. In addition, the electrical sheet resistance does not follow a clear tendency with *P* and *S* values; which evidences the critical correlation between the *S–P* lasing conditions and the structure of the resulting LIG. In the specific case of our laser, an 11% of the maximum power is optimal for the three substrate pre-treatments to convert into LIG. The $R_{s,\parallel}$ values for the fire-retardant pre-treatments are in the same order of magnitude as the PI reference (in the range of 29.5 to 48.4 $\Omega\ sq^{-1}$ for $R_{s,\parallel}$ and 148.9 to 334.3 $\Omega\ sq^{-1}$ regarding $R_{s,\perp}$ values). While, LIGNIN coating presents the lowest $R_{s,\parallel}$ value, with a very repeatable figure of $8.11 \pm 0.37\ \Omega\ sq^{-1}$ (*S*8%–*P*11% conditions) and is indicative of a higher graphitic contest and connected structure. This value is in the same order of magnitude as the lowest R_s in the literature for bio-based sources derived LIG, which is 3.8 $\Omega\ sq^{-1}$,[58] and outranks other LIG structures reported in the literature. This electrical test are

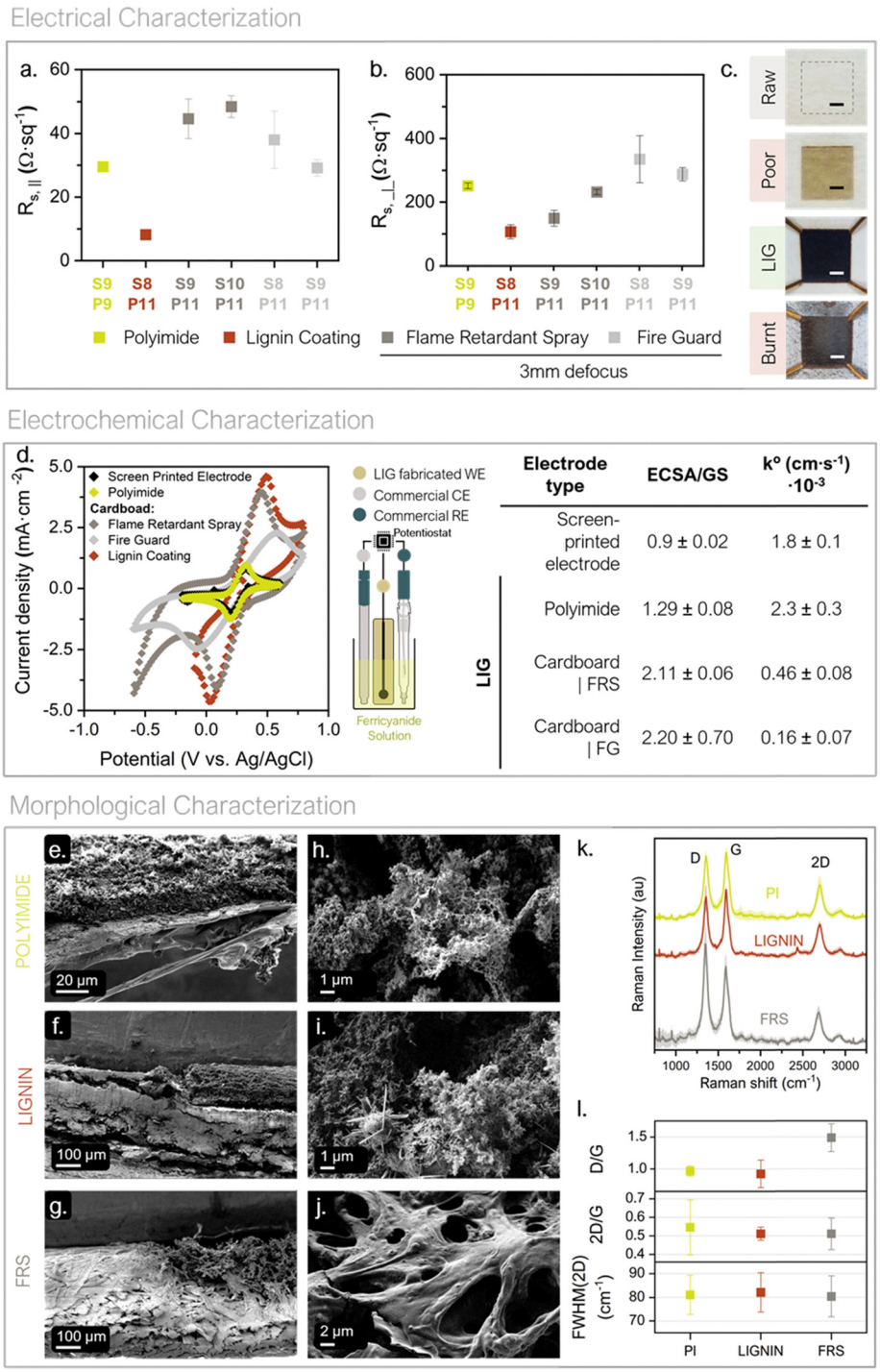

Fig. 2 Electrical, electrochemical and morphological characterization of LIG. Electrical characterization showing sheet resistance values for laser-induced graphene over cardboard precursor with flame retardant spray (RFS) and fire guard (FG) commercial fire retardants (3 mm defocus) and lignin-based coating (LIGNING) as pretreatments. Polyimide (PI) as a reference value (N = 3) Resistance values obtained parallel (a) and perpendicular (b) to the laser raster direction. Optical images of FRS pretreated cardboards before any lasing (''Raw''), after lasing with not LIG leading conditions (''Poor''), after the successful transformation of the precursor into LIG with *S*9%–*P*11% (''LIG''), and after burning the substrate (''Burnt'') (c). Electrochemical characterization, comparison of LIG suitability as electrodic surface *via* cyclic voltammetry (d). Table on the computed electroactive surface area (ECSA) *vs.* geometrical surface (GS) ratio and on the electron transfer rate constant (k°). Screen printed electrode (SPE) as a comparison. Experiment performed with a 3-electrode cell in a beaker with 0.01 M ferricyanide, 1 M KCl at 20 mV scan rate (WE: working electrode, CE: counter electrode, and RE: reference electrode). Morphological characterization showing SEM images for a cross-section of the engraved substrate and high-magnification for each of the material types: PI (e) and (h), LIGNIN-coated cardboard (f) and (i) and FRS-coated cardboard (g) and (j) Represented in (k) is the average Raman spectra from the LIG on the PI, from the LIGNIN and from the FRS pretreated cardboard substrates. The shading represents the standard deviation. D/G ratio, 2D/G ratio and the 2D FWHM of the LIG on each substrate calculated from the spectra in (k) are shown in (l).

evidence that the commercial fire retardant previously used to obtain LIG on organic substrates can be successfully substituted by a bio-based LIGNIN coating, for organic substrates. They also reflect that the fabrication of low sheet resistance LIG is possible in ambient conditions.[55]

2.2.3. Electrochemical characterization. Once the method for LIG generation has been validated, the LIG suitability as electrode surface was assessed. Electrodes with an area of π cm^2, were engraved over the precursor materials. The LIG surfaces' response as a working electrode was tested *via* cyclic voltammetry (CV) using potassium ferrocyanide. A pre-activated carbon screen-printed electrode (SPE) was employed as a control. The responses comparison is depicted in Fig. 2d.

As a first remark, LIG surfaces show good capability for electron exchange in a redox reaction. The voltammogram of LIG over PI has similar electrochemical behavior as the SPE, with a slightly higher current reduction peak, at 0.2 V *vs.* Ag/AgCl. Cardboard electrodes, on the other hand, deliver between two to four times the SPE's current density and show bigger capacitive currents; as expected from the tridimensional-porous nature later observed on SEM images. To further study LIG behavior as an electrode, CV experiments were performed at increasing scan rates, to calculate the electroactive surface area (ECSA) *via* Randles–Ševčík equation (see eqn (S2) and (S3), ESI†) and the electron transfer rate constants (k°) *via* Nicholson method.[59–61] The computed ECSA has been compared with the geometrical electrode area (GA) obtaining a ratio that reflects the surface structure of the electrode. The LIG on the LIGNIN precoated samples was discarded for this electrochemical analysis because it gradually loses mechanical stability when soaked in the beaker solution.

Electrodes engraved on top of cardboard with fire retardant reveal the 3D structure of the LIG, since ECSA/GA rate >1. Albeit lessened, a rough surface can also be concluded for electrodes engraved on polyimide. A 3D structure increments the total available surface for the redox reaction to take place and improves the transport of redox species to the electrode surface. Thus, it is an advantageous property when assembling the electrodes in a galvanic cell, since it will increase the energy density and reduce the internal resistance of the system, providing all in all a more efficient electrochemical system. Regarding the computed k°, all values are between 10^{-3} and 10^{-4} cm s^{-1}, which is within referential order of magnitude for standard glassy carbon under similar concentrations of ferricyanide. From a quick comparison between fire retardants, it can be observed that LIG cardboard electrode pretreated with FRS has a higher k° than pretreated with FG, being $4.6 \pm 0.8 \times 10^{-4}$ and $1.6 \pm 0.7 \times 10^{-4}$ cm s^{-1}, respectively. Furthermore, the LIG shape definition on the cardboard surface with FRS greatly surpasses that achieved with FG (see the border definition comparison on the images in Fig. S5, ESI†). Thus, from here on the FRS pretreatment was prioritized for continuing the experimentation.

Despite LIG has been explored in a wide range of applications, studies about its electrochemical properties still remain scarce in the literature. Thus, these results contribute to the gradual creation of this background knowledge, validating the successful creation of a useful 3D surface electrode over a cardboard substrate.

2.2.4. Morphological characterization. The selected LIG materials were morphologically characterized *via* SEM and Raman spectroscopy, the obtained results are shown in Fig. 2e–l. First, the thicknesses of the LIG from different precursor materials and lasing conditions were estimated by analyzing the cross-section of SEM images (Fig. 2e–g). As expected from the ESCA analysis, the thickness of the LIG on the carboard-derived substrates is larger than that of the LIG obtained from PI substrate (FRS: 182 ± 11 μm, FG: 164 ± 9 μm, LIGNIN: 171 ± 3 μm, PI: 38 ± 1 μm). Based on these measurements and on the earlier sheet resistance characterization, the resistivity of the LIG from the fire retardants pretreated cardboards, from the LIGNIN coating and from the PI was calculated to be 0.48-0.88 Ω cm, 0.14 Ω cm and 0.11 Ω cm, respectively. Analyzing LIG morphology more in deep, in high-magnification images (shown in Fig. 2h–j) it can be observed that LIG morphology presents a porous structure that varies depending on the precursor material. It is noteworthy that, as can be observed in Fig. 2i, the LIGNIN pre-treatment leads to the formation of long-filamented LIG nanostructures that may be responsible for its low sheet resistance. The low magnification imaging of LIG (Fig. S6, ESI†) reveals the traces that result from the rater direction of the laser, they are evidence of the anisotropic nature of LIG, and support the differences in the sheet resistance according to the parallel and perpendicular orientations.

The Raman spectra from the PI, LIGNIN and FRS substrates changed from showing no band before lasing (see Fig. S7, ESI†) to showing bands around 1590 cm^{-1} (G), 2700 cm^{-1} (2D) and at 1350 cm^{-1} (D) that match the signature of LIG (Fig. 2k).[62] The similarity of the 2D/G ratios, and the full-width at half-maximums (FWHM) of the 2D band across precursors reflect the high degree of graphitization after the optimization of the lasing conditions (see Fig. 2l). Ratios around these values are also compatible with the fiber-like LIG, observed in the LIGNIN-pretreated samples.[63] The smaller standard deviation of the 2D/G ratio on the LIGNIN and FRS-coated substrates should relate to a more homogeneous graphitization of the LIG on these samples. The higher D/G ratio of the LIG on the FRS pretreated sample suggests a higher density of defects on these materials and is compatible with a higher density of graphene edges associated to the more porous structure as observed in the related SEM images (Fig. 2j).

2.2.5. Ionically conductive biopolymer as battery matrix. As part of the battery ecodesign process, naturally abundant bio-polymers were chosen to constitute the battery matrix, *i.e.* ion exchange membrane and gelified electrolytes. Carboxymethyl cellulose (CMC) is a cellulose derivative with carboxymethyl groups (–CH_2COOH) added to the polymer chain. CMC has been widely applied in the literature to synthesize bio-based hydrogels. When dissolved it becomes negatively ionized, being able to create physical crosslinking and enhancing the mechanical properties of the hydrogel. On the other side, sodium alginate (AL) is a well-known edible polysaccharide used as a gelling agent in the food industry. It is present in

brown algae cell walls, from which it can be refined. Its gelation property is related to the substitution of sodium ions by cations present in the aqueous media. In the context of this work, the CMC : AL synthesized hydrogel is particularly required to meet certain properties to be suitable as battery matrix, such as high ionic conductivity and good chemical and mechanical stability.

Resulting from the selection of the polymers, hydrogel membrane preparation could be performed with non-toxic reactants using mild gelation conditions by a low-energy demanding solvent casting method. This manufacturing process is directly implementable on roll-to-roll fabrication (see Fig. S2, ESI†). Five membranes with different CMC : AL ratios were synthesized (0 : 100, 25 : 75, 50 : 50, 75 : 25, 100 : 0) using glycerol as a plasticizer (an example of the 75 : 25 membrane is shown in Fig. 3a). The suitability of the matrices as ion conductive media was electrochemically assessed *via* impedance spectroscopy (EIS) and eqn (S4) (ESI†) was used to compute the ionic conductivities reported in Fig. 3b.

All the obtained values of ionic conductivities are in the range of 10^{-4} S cm^{-1} which is adequate for their use as polymeric electrolytes according to the literature.[64] The conductivity study also reveals that a synergistic effect is created when combining the two biopolymers, resulting in a slight enhancement of the conductivity values. The highest conductivity, 4.6×10^{-4} S cm^{-1}, is reached for the 75CMC:25AL combination. Thus, it was selected as the most appealing blend with two purposes, to reduce the battery's internal resistance and to increment the total cellulose content of the battery to enhance its compatibility with paper and cardboard recycling processes.

2.2.6. Redox species selection and hydrogel adaptation to mixed media conditions. The use of non-toxic species was set as a pre-requisite of the design of the galvanic cell to meet the envisioned battery application and corresponding EoL. Ascorbic acid (AA) and iron nitrate $Fe(NO_3)_3$ were selected as harmless anodic and cathodic redox species because of their good compatibility with bio-based ion exchange membranes.[65] Fig. 4 illustrates how the AA and $Fe(NO_3)_3$ couple shows an open circuit voltage around 1 V and have a suitable kinetic response when using mixed-media conditions.

Hence, in order to enhance the battery voltage working range, the selected hydrogel matrix was tested to extreme pH conditions. When testing the hydrogel matrix compatibility with pH any change in the matrix's stability was observed after the progressive addition of potassium hydroxide (KOH, 1 M) or oxalic acid ($C_2H_4O_4$, 0.25 M), achieving pH 14 and pH 1 matrices. Subsequently, to the addition of the pH tuning salts, the matrix capability to retain the redox species was tested. The hydrogels were doped with AA (0.5 M) and $Fe(NO_3)_3$ (1 M), and the plasticizer content was then increased to 10% glycerol to enhance the hydrogel matrix final conductivity, a strategy that has already been reported.[66–68] As shown in the photographs in Fig. S8 (ESI†) self-standing doped membranes were obtained proving the suitability of the blends as a gelified electrolyte.

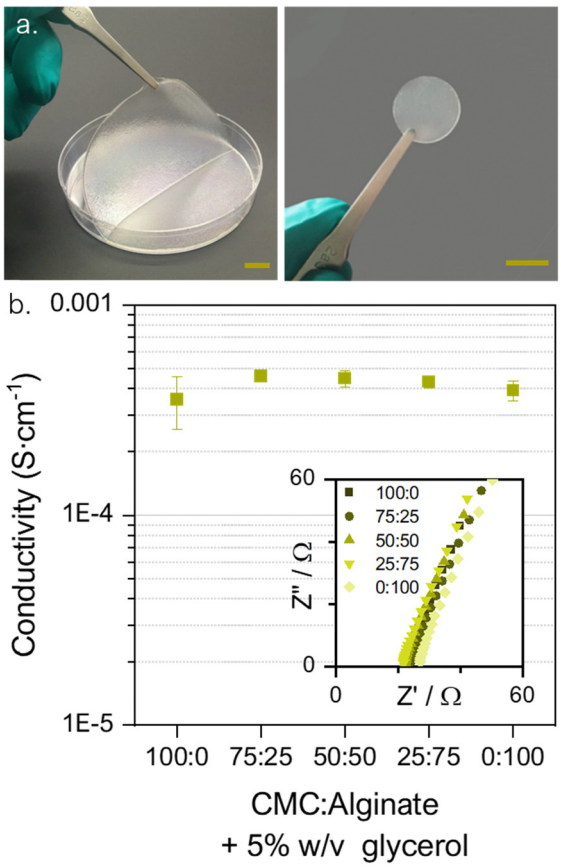

Fig. 3 Self-standing hydrogel membranes from carboxyl-methyl cellulose (CMC) and sodium alginate (AL) with 5% w/v glycerol as a plasticizer. (a) Real photographs of the 75CMC:25AL membrane. Scale bar: 0.5 cm. (b) Ionic conductivity study in relation to the biopolymers ratios and Nyquist plot (inset). N = 3.

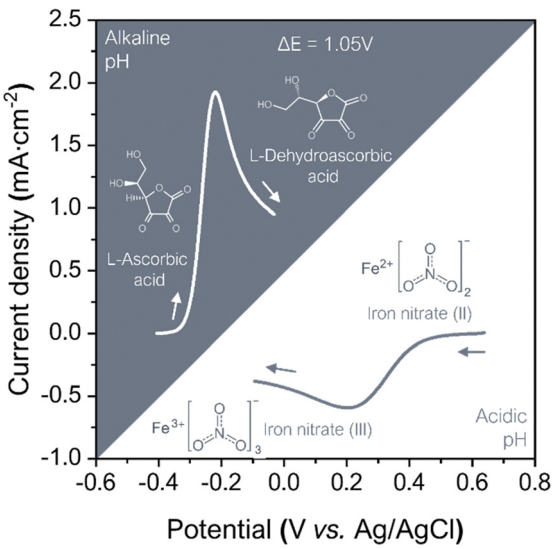

Fig. 4 Linear sweep voltammograms of the redox chemistry couple selected to power the cardboard battery. Oxidation of ascorbic acid (0.01 M) in KOH (1 M) as alkaline electrolyte and reduction of iron nitrate (0.01 M) in $C_2H_4O_4$ (1 M) as acidic electrolyte. Experiment performed with a 3-electrode cell in a beaker, with glassy carbon as working electrode and at 20 mV scan rate.

2.3. Single-cell battery operation

Once all the battery components had been individually developed and validated, the next step was to combine them with the LIG-based current collectors to evaluate the performance of the different materials within an electrochemical galvanic cell. For this purpose, a 25 cm × 20 cm cell prototype was designed and fabricated with LIG-current collectors engraved on cardboard with LIGNIN and FRS as precursor pre-treatments. Again, PI was used as control material. Fig. 5a. shows a battery unit schematic with a complete description of the selected materials and cell geometries.

The cells' performance was electrochemically characterized through polarization curves, sweeping from pre-recorded open circuit voltage (OCV) to 0 V; and continuous discharge was assessed at three externally fixed currents. The plots, in Fig. 5b, demonstrate the feasibility of using LIG engraved on cardboard as current collectors and a bio-based hydrogel matrix in a galvanic electrochemical cell. The OCVs of all recorded functional batteries were between 1.25 and 1.35 V, and maximum power density values of 1.90 ± 0.08 mW cm^{-2} were achieved for cells with LIG-PI current collectors. When using LIG-carboard with FRS as pre-treatment the output power yields almost one order of magnitude less, 0.27 ± 0.02 mW cm^{-2}. This decrease can be directly related to the higher R_s values found for this precursor material (see Fig. 2a). On the other hand, when using LIG-carboard with lignin membrane as coating a maximum power peak of 1.20 ± 0.03 mW cm^{-2} is found. Regarding galvanostatic discharge tests, as expected the higher the delivered currents the shorter the battery service, with a total charge extracted that depends on the pre-fixed discharge currents

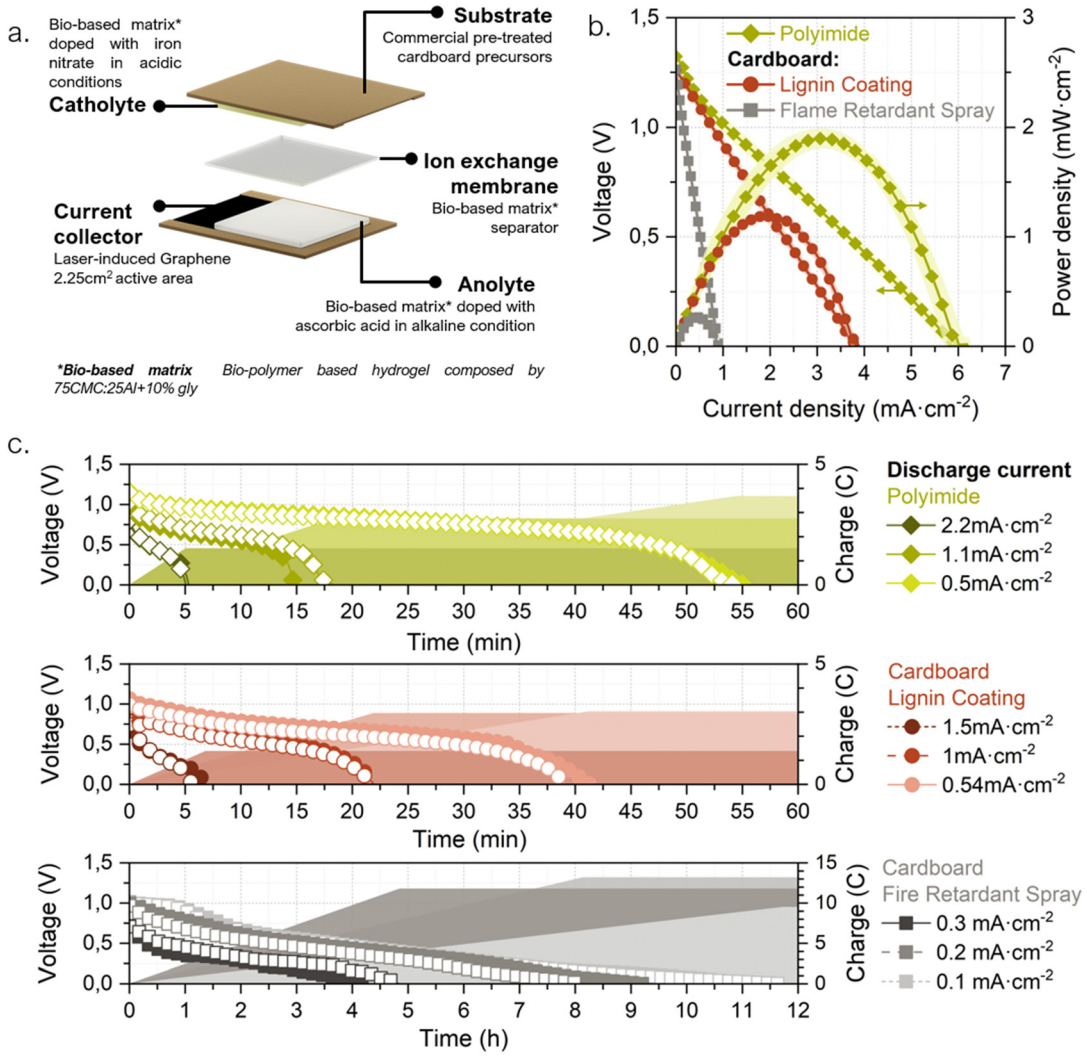

Fig. 5 (a) The schema shows the design and selection of the final materials performed according to the packaging envisioned application and materials screening, characterization and suitability evaluation as battery components. (b) Electrochemical characterization of the single cell battery units *via* polarization curves at 20 mV s^{-1} and (c) galvanostatic discharges at the indicated current in each case. Shaded areas correspond to the accumulated charge over time in relation to each discharge current. The assessment was performed with unitary cells with cardboard-based current collectors generated *via* LIG. Lignin coating and flame-retardant spray cardboard pre-treatments comparison against polyamide as LIG-current collectors. Number of repeats for polarization curves $N \geq 3$, while number of repeats for discharge curves $N = 2$.

(see Fig. 5c). As it can be observed, greater charges are obtained with lower discharge current, *i.e.* longer operation times, indicating that the battery discharge is taking place in the ohmic resistance working regime. Polyimide current collectors delivered currents of 2.2, 1.1 and 0.5 mA cm^{-2} with operational times around 5, 15 and 55 minutes, respectively, and reached 0.43 mA h, 0.69 mA h and 1.03 mA h. For lignin-coating pretreatment current collectors, currents of 1.5, 1.0 and 0.5 mA cm^{-2} were assessed, delivering operational times around 5, 20 and 40 minutes, respectively, and reaching 0.35 mA h, 0.82 mA h and 0.82 mA h total capacities. In the case of FRS pretreatment, due to the higher resistance LIG, lower discharge currents were assessed, thus increasing the operational time to hours. However, despite the same active material load being used, lower demanding currents 0.3, 0.2 and 0.1 mA cm^{-2} delivered lower total capacities of 3.05 mA h, 3.91 mA h and 2.57 mA h, respectively. In light of the results in this section, the selected materials demonstrate a good synergy resulting in a functional galvanic cell with LIG current collectors and a bio-polymeric matrix as the core material used for ionic conduction.

2.4. Smart packaging functional prototype

2.4.1. Energy adaptability. Portable conventional electronics are designed to work with commercially available galvanic cells, such as the well-known lithium coin cells or alkaline batteries. Hence, such applications require power delivered at higher voltages than the one produced by the unitary battery reported above. One extended strategy to obtain higher output voltages from a battery is to stack several cells in series. Stacking designs and their effect on the cell output have been widely reported in the literature.[69] In this work, this same strategy was followed to demonstrate the adaptability of the prototype to different energy requirements. In particular, 2-cell and 4-cell stacks were designed and tested using polyimide as a substrate for LIG engraving, thus validating the technology's scalability. Fig. 6a shows the internal layers configuration and its corresponding electronic circuit representation. As depicted, the cells were internally connected in series using LIG tracks, which avoided the need for any additional electrical components. To minimize the resistance of the intercell connections, the LIG engraving direction was set according to the direction of the connection. As pursued by design, 2-cell and 4-cell stacks achieve open circuit voltages of 2.6 ± 0.02 V and 5.2 ± 0.09 V, respectively (see Fig. 6b). In terms of power peak, the 2-cell and 4-cell stacks yield 6.0 ± 0.2 mW and 11.1 ± 0.9 mW, respectively. Discrepancies in the theoretical output current of the stacks are due to the intercell connection resistance, which can be observed in the increased slope of the *I–V* curve (91.2 ± 0.1 Ω for the single cell, 260.6 ± 0.2 Ω for the 2-cell stack and 612.3 ± 0.2 Ω for the 4-cell stack). This internal resistance causes the 4-cell stack to enter a regime in which mass transport limitations can be evidenced (at operating stack voltages below 0.7 V).[70]

2.4.2. Prototype fabrication and proof-of-concept tests. The battery technology in this article aims to be completely aligned with the packaging industry. For this reason, the final design and fabrication of the prototype were conceived in compliance with the fabrication methods of adhesive labels at an industrial scale, *i.e.* a casting technique to create flexible films and lamination processes to join the different layers together. The interested reader can find a more detailed explanation of label fabrication methods in Fig. S2 (ESI†). Likewise, Fig. S8 (ESI†) shows the layers forming the final prototype, for both single-cell and 4-stack configurations. The lignin membranes developed in the previous sections were used as the substrate to engrave the LIG current collectors. A commercial recyclable adhesive tape serves as the prototype casing and as support

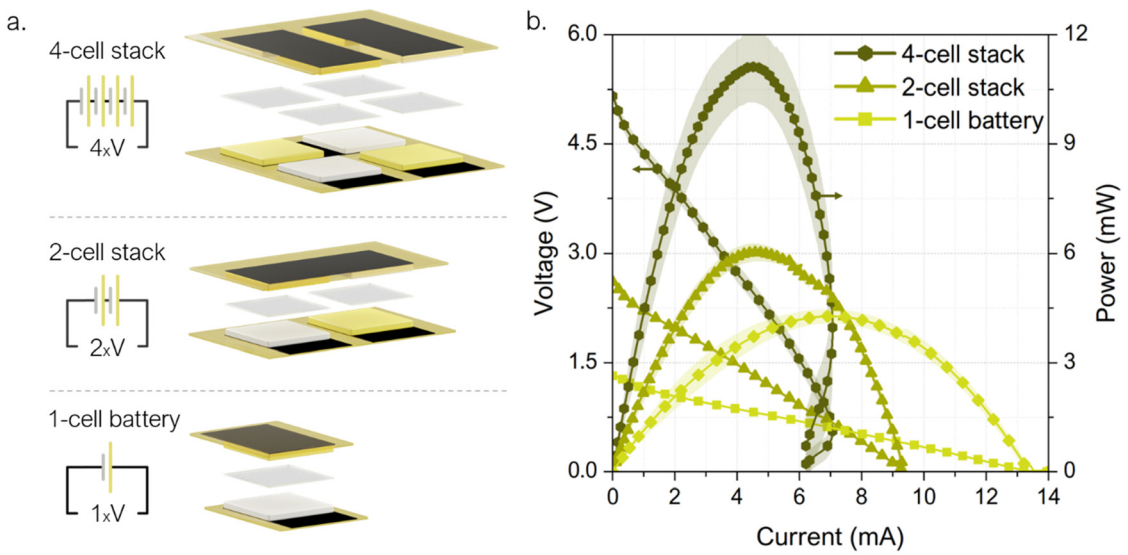

Fig. 6 Demonstration of voltage scalability of the battery. (a) Illustration of the integration of two and four cells in comparison with the one-cell battery and its complementary electronic circuit. Cells are connected in series using LIG paths as current collectors and cell interconnections. (b) Average polarization curves ($N \geq 2$).

material. The previously tested hydrogel matrices (*i.e.* anode, cathode and separator) were incorporated as described before into the final prototypes.

A printed electrochromic display was directly connected to the single-cell prototype, and the battery voltage was recorded while powering ON and OFF the display several times. This cost-effective, ultra-low-power display technology is becoming a new standard for increasing visibility and transparency in several applications within the packaging industry, such as cold chain and logistics monitoring.[71] As it can be observed in Fig. 7 the cell voltage decays from 1.2 V to 0.95 V while transferring charge to the display and once the display is completely turned ON, the cell rapidly recovers to the initial OCV value. The performance of the 4-cell stack was demonstrated by powering a commercial tracking device. The Smart Tracker is a low-cost wireless locator which enables the geolocalization of an object through a smartphone *via* Bluetooth protocol for transferring signals. Generally powered by a primary 3 V coin cell (*i.e.* lithium battery model CR2032), the commercial circuit controlling the tracker was adapted by adding a 10 mF capacitor capable to damp any punctual power fluctuation. Fig. 7 shows the tracker powered directly by the 4-cell stack, without any ancillary power conversion systems. The voltage evolution shows first the battery's capability to fully charge the capacitor, which takes 190 s until the system reaches a final voltage of 4.5 V (see ① in Fig. 7). Then, the tracker was connected and the voltage dropped to 3.5 V while powering the device start-up (see ②) and sending a signal to the smartphone app reporting its activation. Once activated, the tracker entered in an idle mode with minimal energy consumption, while the battery proved to be able to recharge the capacitor back to almost the initial voltage, 4.3 V. The device can thereby stay activated as long as needed. To enable the smartphone-tracker communication the tracker button was pressed twice (see ③). The connection event is shown as a 44 mV drop, from which the battery recovers in a few seconds. In this scenario, the 4-cell stack prototype is shown to reliably deliver the required levels of electrical power to drive off the start-up, idle mode and smartphone-tracker communication.

These experiments serve to demonstrate the prototype design's adaptability to different energy-demanding real-world scenarios, showing the potentiality of the tailored power-source concept.

2.4.3. Recyclability assessment. From the beginning of the battery life-cycle conceptualization, conferring the prototype the capability of being recyclable within the paper and cardboard waste stream was set as the main decision-making driver (recyclable is used here in compliance with the technical definition established in norm UNE-EN 13430). For this reason, to test the feasibility of the proposed end-of-life, it is imperative to demonstrate the compatibility of the final prototype with paper and cardboard waste stream. Hence, the 4-cell stack battery was analyzed using the ATICELCA® 501/19 methodology, which enables the evaluation of the recyclability level of cellulosic materials and products at an industrial level.[72,73] In a nutshell, the method simulates the main phases of the industrial procedures for paper and cardboard recycling, at a laboratory level. Then, it analyses, under the standard UNI 11743: 2019, the parameters related to each procedure phase, namely gross waste measurement and macrostickies and flake content evaluation in the recovered paper pulp. Finally, it performs adhesive particle determination and optical assessment of inhomogeneities in the produced recycled paper sheet.

The 4-cell stack prototype was evaluated in a real-world scenario, by attaching it to two typical packaging products, a cardboard box (25 cm × 15 cm × 10 cm, 80 g, 350 g m^{-2}) and a cardboard envelope (A4, 90 g, 450 g m^{-2}). Table 1 shows the results of the paper and cardboard recycling compatibility assessment for the cardboard box and envelope with and without the attached prototype.

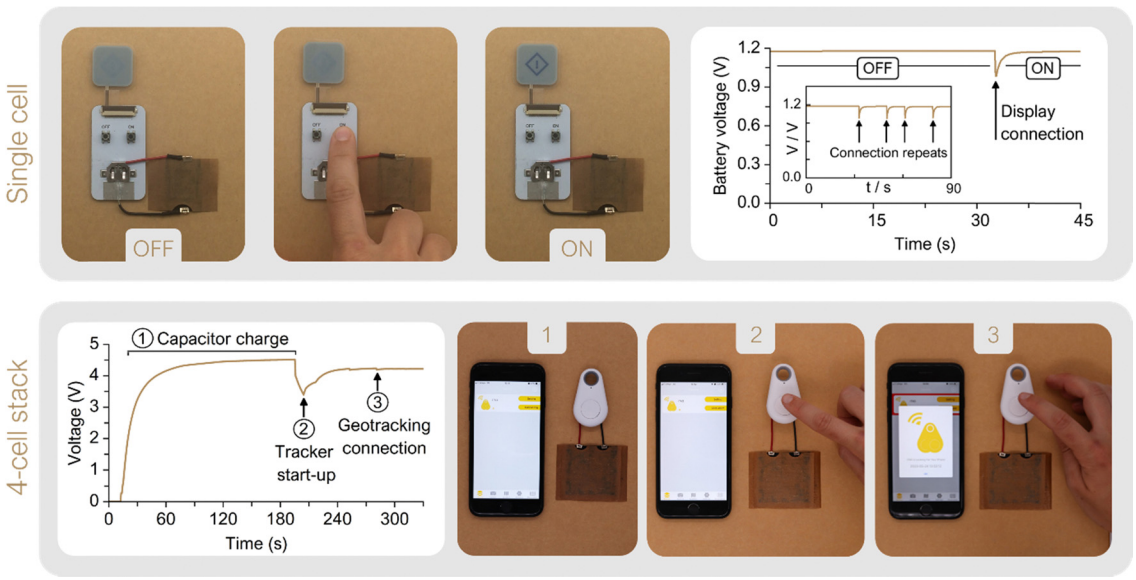

Fig. 7 Proof of concept of the battery energy adaptability demonstrating the capability of powering an electrochromic display (single-cell battery) and the start-up, idle mode and bluetooth connection of a tracker device (4-cell stack battery).

Table 1 Battery recyclability with paper and cardboard. The assessment was performed according to UNI 11743:2019 standard using ATICEL 501/19 methodology. Gathered in the table are the values for the gross waste percentage, the total macrostickies content and the total macrostickies with a diameter smaller than 2000 μm, in $mm^2\ kg^{-1}$. The values for the percentage of fiber flakes presence and the recycled paper sheet stickiness and optical inhomogeneities analysis are also collected. Values reported for a cardboard box and an envelope with and without the presence of 4-cell stack battery prototype

	Cardboard BOX	Envelope	Cardboard box + prototype	Envelope + prototype
Gross waste (%)	0.11	1.18	1.40	1.42
Macrostickies ($mm^2\ kg^{-1}$)				
Total area	4825.95	15 334.96	29 396.00	25 904.10
Area for $\phi < 2000$ μm	3386.11	8011.78	21 007.54	25 272.78
Fibers flakes (%)	3.61	4.39	4.70	1.84
Paper sheet analysis				
Adhesivity	Absent	Absent	Absent	Absent
Inhomogeneities	Not observed	Not observed	Not observed	Not observed

The found values do not exceed in any case the limit values imposed by the norm (gross waste > 40%, macrostickies ($\phi < 2000$ μm) > 50 000 $mm^2\ kg^{-1}$ or stickiness presence in the paper sheet). Therefore, according to the norm, the prototype end-of-life is completely aligned with the common practices in the intended application sector and can be directly managed within the paper and cardboard waste steam without causing a disturbance in the common industrial processes. Although it is beyond the scope of this work, it is worth mentioning that further studies would be needed to determine the fate of the battery materials that have no cellulosic nature, the possibility to recover them from the paper recycling stages (*e.g.* from recovered pulp or black liquor) and to assess the environmental impact of these components.

3. Experimental methods

Despite the experimental protocols have been briefly described in the main text, a more detailed description of all materials and methods has been included in the ESI.†

4. Conclusions

The Internet of Things is set out to be one of the upcoming technology revolutions. At the same time, waste electrical and electronic equipment is currently the fastest-growing waste stream, and only a fraction is managed in a systematic and environmentally responsible way including the recovery of valuable materials. In this context, the portable battery concept presented herein advocates and showcases a technological innovation with strong priorities refocusing. In this study, the battery has been designed by purpose to power IoT devices in the smart-packaging sector. The intended application has been placed as the linchpin to guide a life cycle thinking approach for the definition of the selection of materials, the design of the fabrication processes and the EoL. Directly embedding the recyclability criteria of the host product in the design process of the power source. Laser induced graphene is applied as the carbon-based current collector material. A hydrogel matrix, created by combining sodium alginate and CMC, acts as the electrode separator and contains the non-toxic redox species. Finally, a commercial recyclable cardboard tape is successfully used as a battery backing and casing. Furthermore, the conferred adhesive label format ensures an easy implementation to the envisioned application sector.

The matching of power performance and sustainability criteria, through the customization of the battery prototype to a specific application, results in efficient use of materials and tailors the stored energy to different power requirements. In this sense, the prototype's practicality was validated by powering two exemplary applications for the smart packaging sector: a printed electrochromic display and a wireless tracker device. Ultimately, the battery is proven to be compatible with paper and cardboard recycling processes under the standardized norm. This unconventional End-of-Life for a battery represents an alternative solution for ensuring the power source's correct management, preventing potential environmental risks while overcoming the need for separate collection and treatment routes which cause high efforts and environmental impacts.

The presented methodology considers relevant aspects that facilitate the industrial scale-up of a technology from an early conceptual stage, including criteria to define the materials and product design based on environmental sustainability considerations, economic viability and manufacturability. These validations should then be performed continuously and iteratively as the technology moves forward in readiness level.

Correspondingly, the versions of the demonstrator need to be further investigated, upscaled and quantitatively evaluated in a comprehensive prospective sustainability assessment, including life cycle assessment, life cycle costing and social-life cycle assessment. Only in this case, a comprehensive picture can be provided for further environmentally conscious improvement of the technology.

Author contributions

Navarro-Segarra: conceptualization, methodology, validation, formal analysis, investigation, writing – original draft, writing – review & editing, visualization, supervision. O. A. Ibrahim: conceptualization, writing – original draft, writing – review & editing funding acquisition. I. Martin-Fernandez: formal analysis, investigation, writing – original draft, writing – review &

editing. C. Tortosa: methodology, validation, formal analysis, investigation, writing – original draft, visualization. J. M. Ormaetxea: validation, formal analysis, investigation, data curation, writing – original draft. M. Baumann: writing – review & editing, resources, supervision. M. Weil: writing – review & editing, resources, supervision, project administration, funding acquisition. J. P. Esquivel: conceptualization, methodology, writing – review & editing, resources, supervision, project administration, funding acquisition.

Conflicts of interest

There are no conflicts to declare.

Acknowledgements

The authors would like to thank the Cluster of Excellence POLiS (which is funded by the German Research Foundation (DFG) under Project ID 390874152) for the Early Career Researchers award received for this work and the financial support from Marie Skłodowska-Curie European Fellowships within the European Union's H2020 Framework Programme (grant agreements: 101033075-SPRICE and 665919−P-SPHERE). This work has also been partially funded by Generalitat de Catalunya-AGAUR (2021 SGR 00497). Furthermore, the authors would like to express their gratitude to UBIS company for their donation of recyclable tape KRAFT 700 and for their invaluable explanations about the technologies behind the packaging sector. The authors also thank David Batet for his help on SEM analysis, Andrea Ugalde for her involvement in battery current collectors' fabrication, Dr Narcís Mestres for his support with Raman spectroscopy and Joan Garcia and Mireia Laplaza for conducting preliminary experimentation.

Notes and references

1 W. E. Forum, Digital Transformation of Industries: Societal Implications, https://www.weforum.org/publications/digital-transformation-of-industries/.
2 A. K. Feroz, H. Zo and A. Chiravuri, *Sustainability*, 2021, **13**, 1–20.
3 C. Santato and P.-J. Alarco, *Adv. Mater. Technol.*, 2022, **7**, 2101265.
4 V. Forti, C. P. Baldé, R. Kuehr and G. Bel, *The Global E-waste Monitor 2020*, 2020.
5 G. Rodriguez-Garcia and M. Weil, in *WEEE Recycling*, ed. A. Chagnes, G. Cote, C. Ekberg, M. Nilsson and T. Retegan, Elsevier, 2016, pp. 177–207.
6 W. E. Forum, The world's e-waste is a huge problem. It's also a golden opportunity, https://www.weforum.org/agenda/2019/01/how-a-circular-approach-can-turn-e-waste-into-a-golden-opportunity/.
7 WHO, Soaring e-waste affects the health of millions of children, https://www.who.int/news/item/15-06-2021-soaring-e-waste-affects-the-health-of-millions-of-children-who-warns.
8 W. E. Forum, A New Circular Vision for Electronics, Time for a Global Reboot, https://www.weforum.org/publications/a-new-circular-vision-for-electronics-time-for-a-global-reboot/.
9 J. F. Peters, M. Baumann, J. R. Binder and M. Weil, *Sustainable Energy Fuels*, 2021, **5**, 6414–6429.
10 McKinsey Global Institute, *The Internet of Things: Catching up to an accelerating opportunity*, 2021.
11 M. G. Institute, *McKinsey & Company*, 2015, pp. 1–18.
12 S. S. Sharma and A. Manthiram, *Energy Environ. Sci.*, 2020, **13**, 4087–4097.
13 D. Sherwood, *A water fight in Chile's Atacama raises questions over lithium mining*, 2018, access 21/02/2024.
14 D. Baumann-Pauly, Geneva Center for Business and Human Rights and NYU Stern Center for Business and Human Rights, 2023.
15 A. Koyamparambath, J. Santillán-Saldivar, B. McLellan and G. Sonnemann, *Resour. Policy*, 2022, **75**, 102465.
16 International Amnesty, *Exposed: Child labour behind smart phone and electric car batteries*, 2016, access 20/04/2024.
17 J. F. Peters and M. Weil, *J. Cleaner Prod.*, 2018, **171**, 704–713.
18 M. Petzold and S. Flamme, *Metals*, 2024, **14**, 151.
19 H. E. Melin, *Circular Energy Storage, commissioned by The Swedish Energy Agency*.
20 L. Gaines, J. Zhang, X. He, J. Bouchard and H. E. Melin, *Batteries*, 2023, **9**, 360.
21 J. Lin, X. Zhang, E. Fan, R. Chen, F. Wu and L. Li, *Energy Environ. Sci.*, 2023, **16**, 745–791.
22 E. parliament and the C. of the E. Union, REGULATION (EU) 2023/1542, https://eur-lex.europa.eu/legal-content/EN/TXT/PDF/?uri=CELEX:32023R1542.
23 Eurostat, *eurostat*, 2020, pp. 1–14.
24 E. C. E. Directorate-General, *Making sustainable consumption and production a reality: a guide for business and policy makers to life cycle thinking and assessment*, Publications Office of the European Union, 2010.
25 SMITHERS, The Future of Packaging: Long-Term Strategic Forecast to 2028, https://www.smithers.com/resources/2019/feb/future-packaging-trends-2018-to-2028.
26 D. Schaefer and W. M. Cheung, in *Procedia CIRP*, Elsevier, 2018, vol. 72, pp. 1022–1027.
27 S. Yildirim, B. Röcker, M. K. Pettersen, J. Nilsen-Nygaard, Z. Ayhan, R. Rutkaite, T. Radusin, P. Suminska, B. Marcos and V. Coma, *Compr. Rev. Food Sci. Food Saf.*, 2018, **17**, 165–199.
28 European Portable Battery Association|What is a battery? https://www.epbaeurope.net/portable-batteries/portable-batteries-primary-batteries-rechargeable-batteries-consumer-batteries/.
29 C. M. Costa, R. Gonçalves and S. Lanceros-Méndez, *Energy Storage Mater.*, 2020, **28**, 216–234.
30 B. Clement, M. Lyu, E. Sandeep Kulkarni, T. Lin, Y. Hu, V. Lockett, C. Greig and L. Wang, *Engineering*, 2022, **13**, 238–261.

31 European Commission, *Directorate General for Internal Market, Industry, Entrepreneurship and SMEs., Study on the critical raw materials for the EU 2023: final report*, Publications Office, LU, 2023.
32 D. Laura, Guidance on Key Considerations for the Identification and Selection of Safer Chemical Alternatives, **https://www.oecd.org/chemicalsafety/risk-management/guidance-on-key-considerations-for-the-identification-and-selection-of-safer-chemical-alternatives.pdf**.
33 M. Baumann, M. Häringer, M. Schmidt, L. Schneider, J. F. Peters, W. Bauer, J. R. Binder and M. Weil, *Adv. Energy Mater.*, 2022, **12**, 2202636.
34 European Critical Raw Materials Act, **https://ec.europa.eu/commission/presscorner/detail/en/ip_23_1661**, (accessed 24 May 2024).
35 M. Z. Hauschild, S. Kara and I. Røpke, *CIRP Ann.*, 2020, **69**, 533–553.
36 K. Ramani, D. Ramanujan, W. Z. Bernstein, F. Zhao, J. Sutherland, C. Handwerker, J.-K. Choi, H. Kim and D. Thurston, *J. Mech. Design*, 2010, **132**, 091004.
37 M. Haase, C. Wulf, M. Baumann, C. Rösch, M. Weil, P. Zapp and T. Naegler, *Energy Sustainability Soc.*, 2022, **12**, 20.
38 M. Erakca, M. Baumann, C. Helbig and M. Weil, *J. Cleaner Prod.*, 2024, **451**, 142161.
39 M. Navarro-Segarra and J. P. Esquivel, *Sustainable Energy Storage in the Scope of Circular Economy*, John Wiley & Sons, Ltd, 2023, pp. 123–143.
40 Y. Umeda, S. Takata, F. Kimura, T. Tomiyama, J. W. Sutherland, S. Kara, C. Herrmann and J. R. Duflou, *CIRP Ann.*, 2012, **61**, 681–702.
41 Chemicals strategy – European Commission, **https://environment.ec.europa.eu/strategy/chemicals-strategy_en**, (accessed 24 May 2024).
42 S. Dühnen, J. Betz, M. Kolek, R. Schmuch, M. Winter and T. Placke, *Small Methods*, 2020, **4**, 2000039.
43 G. S. D. Reis, S. H. Larsson, H. P. de Oliveira, M. Thyrel and E. C. Lima, *Nanomaterials*, 2020, **10**, 1–22.
44 A. J. S. Ahammad, J. J. Lee and M. A. Rahman, *Sensors*, 2009, **9**, 2289–2319.
45 P. Zhu, D. Gastol, J. Marshall, R. Sommerville, V. Goodship and E. Kendrick, *J. Power Sources*, 2021, **485**, 229321.
46 D. A. C. Brownson and C. E. Banks, *The Handbook of Graphene Electrochemistry*, Springer, 2014.
47 R. Ye, D. K. James and J. M. Tour, *Adv. Mater.*, 2019, **31**, 1803621.
48 J. Liang, A. K. Mondal, D. W. Wang and F. Iacopi, *Adv. Mater. Technol.*, 2019, **4**, 1800200.
49 J. Lin, Z. Peng, Y. Liu, F. Ruiz-Zepeda, R. Ye, E. L. G. Samuel, M. J. Yacaman, B. I. Yakobson and J. M. Tour, *Nat. Commun.*, 2014, **5**, 1–8.
50 G. Chen, Y. Liu, F. Liu and X. Zhang, *Appl. Surf. Sci.*, 2014, **311**, 808–815.
51 M. Ren, J. Zhang and J. M. Tour, *ACS Appl. Energy Mater.*, 2019, **2**, 1460–1468.
52 Y. Li, D. X. Luong, J. Zhang, Y. R. Tarkunde, C. Kittrell, F. Sargunaraj, Y. Ji, C. J. Arnusch and J. M. Tour, *Adv. Mater.*, 2017, **29**, 1700496.
53 Y. Chyan, R. Ye, Y. Li, S. P. Singh, C. J. Arnusch and J. M. Tour, *ACS Nano*, 2018, **12**, 2176–2183.
54 W. Ma, J. Zhu, Z. Wang, W. Song and G. Cao, *Mater. Today Energy*, 2020, **18**, 100569.
55 R. Ye, Y. Chyan, J. Zhang, Y. Li, X. Han, C. Kittrell and J. M. Tour, *Adv. Mater.*, 2017, **29**, 1702211.
56 F. Mahmood, C. Zhang, Y. Xie, D. Stalla, J. Lin and C. Wan, *RSC Adv.*, 2019, **9**, 22713–22720.
57 W. Zhang, Y. Lei, F. Ming, Q. Jiang, P. M. F. J. Costa and H. N. Alshareef, *Adv. Energy Mater.*, 2018, **8**, 1–9.
58 J. Edberg, R. Brooke, O. Hosseinaei, A. Fall, K. Wijeratne and M. Sandberg, *npj Flexible Electron.*, 2020, **4**, 1–10.
59 R. S. Nicholson, *Anal. Chem.*, 1965, **37**, 1351–1355.
60 J. E. B. Randles, *Trans. Faraday Soc.*, 1948, **44**, 327–338.
61 A. Ševčík, *Collect. Czech. Chem. Commun.*, 1948, **13**, 349–377.
62 A. C. Ferrari and D. M. Basko, *Nat. Nanotechnol.*, 2013, **8**, 235–246.
63 V. D. Li, J. T. Li, J. L. Beckham, W. Chen, B. Deng, D. X. Luong, C. Kittrell and J. M. Tour, *Adv. Funct. Mater.*, 2022, **32**, 2110198.
64 E. Lizundia and D. Kundu, *Adv. Funct. Mater.*, 2021, **31**, 2005646.
65 P. P. Alday, S. C. Barros, R. Alves, J. M. S. S. Esperança, M. Navarro-Segarra, N. Sabaté, M. M. Silva and J. P. Esquivel, *Adv. Sustainable Syst.*, 2020, **4**, 1900110.
66 D. K. Pradhan, R. N. P. Choudhary and B. K. Samantaray, *Int. J. Electrochem. Sci.*, 2008, **3**, 597–608.
67 L. S. Ng and A. A. Mohamad, *J. Power Sources*, 2006, **163**, 382–385.
68 D. F. Vieira and A. Pawlicka, *Electrochim. Acta*, 2010, **55**, 1489–1494.
69 J. P. Esquivel, P. Alday, O. A. Ibrahim, B. Fernández, E. Kjeang and N. Sabaté, *Adv. Energy Mater.*, 2017, **7**, 1700275.
70 O. A. Ibrahim, M. Navarro-Segarra, P. Sadeghi, N. Sabaté, J. P. Esquivel and E. Kjeang, *Chem. Rev.*, 2022, **122**, 7236–7266.
71 YNVISIBLE, Printed E-paper Display Manufacturer, **https://www.ynvisible.com/**.
72 Associazione tecnica italiana cellulosa e carta, **https://www.aticelca.it/1/riciclabilita-della-carta/**.
73 Ecolstudio, Recyclability of paper The Aticelca® 501 test, **https://www.ecolstudio.com/en/recyclability-paper-aticelca-test**.

